Journal of Atmospheric Chemistry **16**: 313–335, 1993.

Simultaneous Measurements of Peroxy and Nitrate Radicals at Schauinsland

D. MIHELCIC, D. KLEMP, P. MÜSGEN, H. W. PÄTZ, and A. VOLZ-THOMAS
Institut für Chemie und Dynamik der Geosphäre 2, Chemie der Belasteten Atmosphäre, Forschungszentrum Jülich, D-5170 Jülich, Germany

(Received: 28 May 1992)

Abstract. We present simultaneous field measurements of NO_3 and peroxy radicals made at night in a forested area (Schauinsland, Black Forest, 48° N, 8° N, 1150 ASL), together with measurements of CO, O_3, NO_x, NO_y, and hydrocarbons, as well as meteorological parameters. NO_2, NO_3, HO_2, and $\Sigma(RO_2)$ radicals are detected with matrix isolation/electron spin resonance (MIESR). NO_3 and HO_2 were found to be present in the range of 0–10 ppt, whilst organic peroxy radicals reached concentrations of 40 ppt. NO_3, RO_2, and HO_2 exhibited strong variations, in contrast to the almost constant values of the longer lived trace gases. The data suggest anticorrelation between NO_3 and RO_2 radical concentrations at night.

The measured trace gas set allows the calculation of NO_3 and peroxy radical concentrations, using a chemical box model. From these simulations, it is concluded that the observed anthropogenic hydrocarbons are not sufficient to explain the observed RO_2 concentrations. The chemical budget of both NO_3 and RO_2 radicals can be understood if emissions of monoterpenes are included. The measured HO_2 can only be explained by the model, when NO concentrations at night of around 5 ppt are assumed to be present. The presence of HO_2 radicals implies the presence of hydroxyl radicals at night in concentrations of up to 10^5 cm^{-3}.

Key words. HO_2-, RO_2-, and NO_3-radicals, tropospheric measurements, matrix isolation/electron spin resonance, nighttime chemistry.

1. Introduction

Organic peroxy radicals are the most important chain carriers in the oxidation of hydrocarbons. Besides their formation through reactions of hydrocarbons and CO with hydroxyl radicals during daytime, these radicals may also be formed at night, through reactions of hydrocarbons with NO_3 radicals and from the metabolism of Criegee intermediate upon reaction of alkenes with ozone (Atkinson and Lloyd, 1984; Atkinson, 1990).

A schematic diagram of the nighttime chemistry involving NO_3 is shown in Figure 1. NO_3 radicals are produced by reaction of ozone with NO_2. A fast equilibrium is established between NO_3, NO_2, and N_2O_5. Both NO_3 and N_2O_5 can be removed by reactions with hydrometeors, which lead to formation of dissolved NO_3^-, a process which provides a nighttime sink for atmospheric NO_x (Heikes and Thompson, 1983) and, implicitly, O_3 (Volz *et al.*, 1989). In addition, the NO_3 radical reacts with atmospheric hydrocarbons. Whilst its reaction with alkanes is rather slow, the addition to the double bond of alkenes followed by reaction with O_2 to

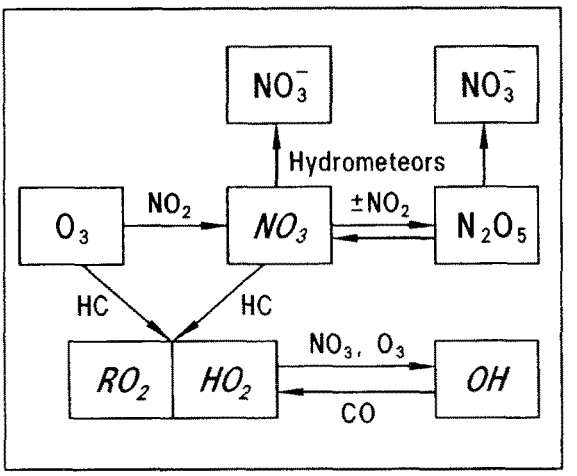

Fig. 1. Simplified scheme of nighttime chemistry of NO_y species.

yield β-nitrato alkylperoxy radicals (Atkinson, 1991 and references therein) proceeds fast enough to make it a potentially important source of RO_2 radicals at night. In particular, the reaction of NO_3 with terpenes is rather fast (rate coefficients of $\geqslant 10^{-12}$ cm^3 molec^{-1} sec^{-1}, Atkinson *et al.*, 1991). NO_3 also reacts with aldehydes to yield RO_2 radicals and nitric acid (Morris and Niki, 1974; Cantrell *et al.*, 1985). As was recently pointed out by Mellouki *et al.* (1988), Hjorth *et al.*, (1990), and Platt *et al.* (1990), reactions of RO_2 with NO_3 lead to the formation of alkoxy radicals (1). Hence, the NO_3 radical can play a similar role as does NO during daytime, namely by initiating chain reactions that lead to the formation of HO_2 and OH radicals at night (2), (3a).

$$RO_2 + NO_3 \rightarrow RO + NO_2 + O_2 \quad (1)$$

$$RO + O_2 \rightarrow R\dagger CHO + HO_2 \quad (2)$$

$$HO_2 + NO_3 \rightarrow OH + NO_2 + O_2 \quad 80\% \quad (3a)$$

$$\rightarrow HNO_3 + O_2 \quad 20\% \quad (3b)$$

Another path for the production of alkoxy radicals and, thus, HO_2 is via permutation reactions of RO_2 radicals (Madronich *et al.*, 1990).

A few rate constants have been reported for reactions (3) (Mellouki *et al.*, 1988) and (1) (Hjorth *et al.*, 1990; Crowley *et al.*, 1990a, 1990b). They range from 3.6×10^{-12} cm^3 molec^{-1} sec^{-1} for HO_2 to 10^{-13} cm^3 molec^{-1} sec^{-1} for $C_2H_5O_2$. Therefore, the quantitative description of radical chemistry at night is still subject of large uncertainty. There exist a few nighttime measurements of RO_2 radical concentrations at Deuselbach a rural site in Germany (Mihelcic *et al.*, 1985). We report here the results of simultaneous measurements of NO_3, HO_2, and organic peroxy radicals, together with measurements of a number of long-lived trace gases, and meteorological parameters. A time-dependent box model was used to understand the behaviour of RO_2 and NO_3 during that night.

2. Experimental

The measurements were made in the night of 24 and 25 August 1990, during a field campaign at our field station Schauinsland, a mountain located in Southern Germany, about 10 km SSE of the city of Freiburg (48° N, 8° E, 1150 m ASL). The station is operated in the context of the EUROTRAC subproject TOR. The continuous measurements include NO, NO_x, NO_y, O_3, CO, H_2O_2, aerosol concentration, $J(NO_2)$ and meteorological parameters (Volz-Thomas *et al.*, 1990, 1991). Measurements of C_2—C_5 hydrocarbons and alkylnitrates are made at ≈ 3 hourly intervals by means of an automated GC (Rudolph *et al.*, 1990; Flocke *et al.*, 1988, 1991).

The concentrations of RO_2, NO_3, and NO_2 radicals were measured by using matrix isolation and electron spin resonance spectroscopy (MIESR), which has been described previously (Mihelcic *et al.*, 1985, 1990). Briefly, the radicals are trapped from ambient air in a polycrystalline D_2O matrix at a temperature of 77 K. The sampling interval is approximately 30 min (8 l STP of ambient air). The sampling efficiency is $\geqslant 95\%$. Both speciation and quantification is achieved after the samples have been brought to the laboratory by electron spin resonance spectroscopy on a *Varian*-E Line spectrometer with a 12 inch magnet and a V4535 cavity. The ESR spectra are analyzed with a recently developed numerical procedure which was demonstrated to allow speciation of NO_2, NO_3, HO_2, $CH_3C(O)O_2$, and the sum of the alkylperoxy radicals (Mihelcic *et al.*, 1990). The detection limit is 5 ppt for HO_2, RO_2, and NO_2 and 3 ppt for NO_3, due to its narrower ESR line width. The accuracy of the whole procedure, as estimated from absolute calibration, is $\pm$ 5%.

The MIESR samples were collected 15 m above ground, the height where the inlets for the continuous measurements are located, in order to avoid direct influence of the surface. For this purpose, the cryosampler was mounted on a pneumatic mast. A ballbearing and a wind vane served to always point the inlet orifice into the wind to avoid contaminations by the sampler itself or the exhaust from the lq.N_2 reservoir. A detailed description of the instrumentation and experimental parameters for the additional measurements performed at Schauinland will be published elsewhere.

Figure 2 gives a typical example of an ESR spectrum recorded from a sample collected during the night of 24 and 25 August 1990. It shows the relative signal intensity (first derivative of ESR absorption spectrum) as a function of magnetic field. The uppermost trace is the original spectrum of the air sample. It is dominated by NO_2, as is evident from comparison with the NO_2 reference spectrum (trace B). The NO_2 concentration in that sample was 0.65 ppbv. Subtraction of NO_2 yields the residual spectrum shown in trace C. It closely matches the hyperfine structure of the NO_3 reference spectrum (trace D). A simultaneous fit of the reference spectra of NO_3, HO_2, $CH_3C(O)O_2$, CH_3O_2, $C_2H_5O_2$, and $C_3H_7O_2$ retrieved concentrations of 9.5 ppt NO_3, whereas the mixing ratios of the different peroxy

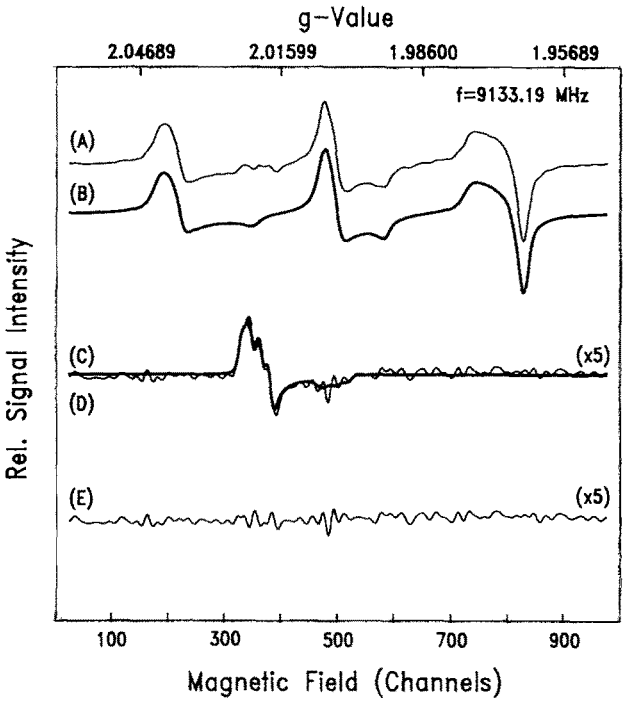

Fig. 2. (A) ESR spectrum of a sample collected on 25 August 1990 at 3:30–4:00 (CET). It was measured at 77 K, with a 2 Gauss modulation amplitude, 200 Gauss scan range, and 60 scan averaged. (B) NO_2 reference spectrum in pure D_2O matrix measured at 77 K, with a modulation amplitude of 2 Gauss, 200 Gauss scan range, and 18 scans averaged. (C) Difference (A–B), magnified by 5. (D) NO_3 reference spectrum in D_2O matrix as retrieved by the fit (magnified by 5). (E) Residuals after subtraction of (D) from (C).

radicals were found to be less than 1 ppt. The relative error of the fit was 30% and the correlation coefficient was 0.96. Trace E shows the residuals after subtraction of the fitted reference spectra.

The spectrum of another sample, which was collected between 22:10 and 22:40 hr, is shown in Figure 3. It is again dominated by NO_2 (0.68 ppb), however, the residual spectrum (trace C) differs significantly from that in Figure 2. Comparison with the reference spectra (trace E(NO_3), F(HO_2), and G(ΣRO_2)) clearly indicates that the residual spectral signature in the atmospheric sample is governed by NO_3 and HO_2. The fit retrieved 5 ppt NO_3, 10 ppt HO_2, and 5 ppt of alkylperoxy radicals with a relative error of 40% and a correlation coefficient of 0.92.

3. Results

Figure 4 shows the concentrations of CO, O_3, NO_y, NO_2, NO_3, HO_2, ΣRO_2, and particles, together with temperature, relative humidity, wind direction, and wind speed during the night from 24 to 25 August 1990. The concentrations of C_2—C_5 hydrocarbons are listed in Table I.

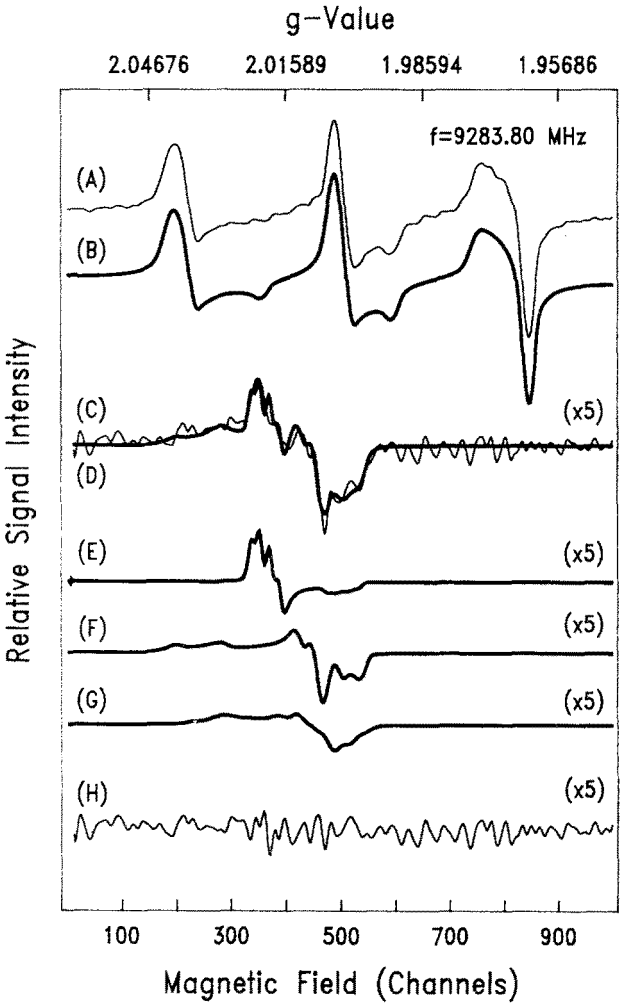

Fig. 3. (A) ESR spectrum of a sample collected on 24 August 1990 at 22:10–22:40 (CET). It was measured at 77 K, with a 2 Gauss modulation amplitude, 200 Gauss scan range, and 60 scans averaged. (B) NO_2 reference spectrum as in Figure 2B. (C) Difference (A-B), magnified by 5. (D) Sum of NO_3 (5.2 ppt), HO_2 (10 ppt), alkyl peroxy radicals (5 ppt) as retrieved by the fit (magnified by 5). (E), (F), (G) Portions of NO_3, HO_2, and ΣRO_2 (all magnified by 5), as retrieved by multiple fit. (H) Residuals after subtraction of (D) from (C).

As is seen from the sharp drop of the concentrations of aerosols, NO_y, and NO_2, an inversion below the site established in the late afternoon around 19:00 hr, which shielded the Schauinsland from the pollution sources in the Rhine Valley underneath. This situation is typical for the Schauinsland during the persistence of a high pressure system (Geiß *et al.*, 1992). Winds were from SW with wind speeds slowly increasing from 2 to 4 m sec^{-1} and the temperature slowly decreasing from 20.7 to 18.5 °C. Relative humidity (RH) increased from 48 to 56% during the time when

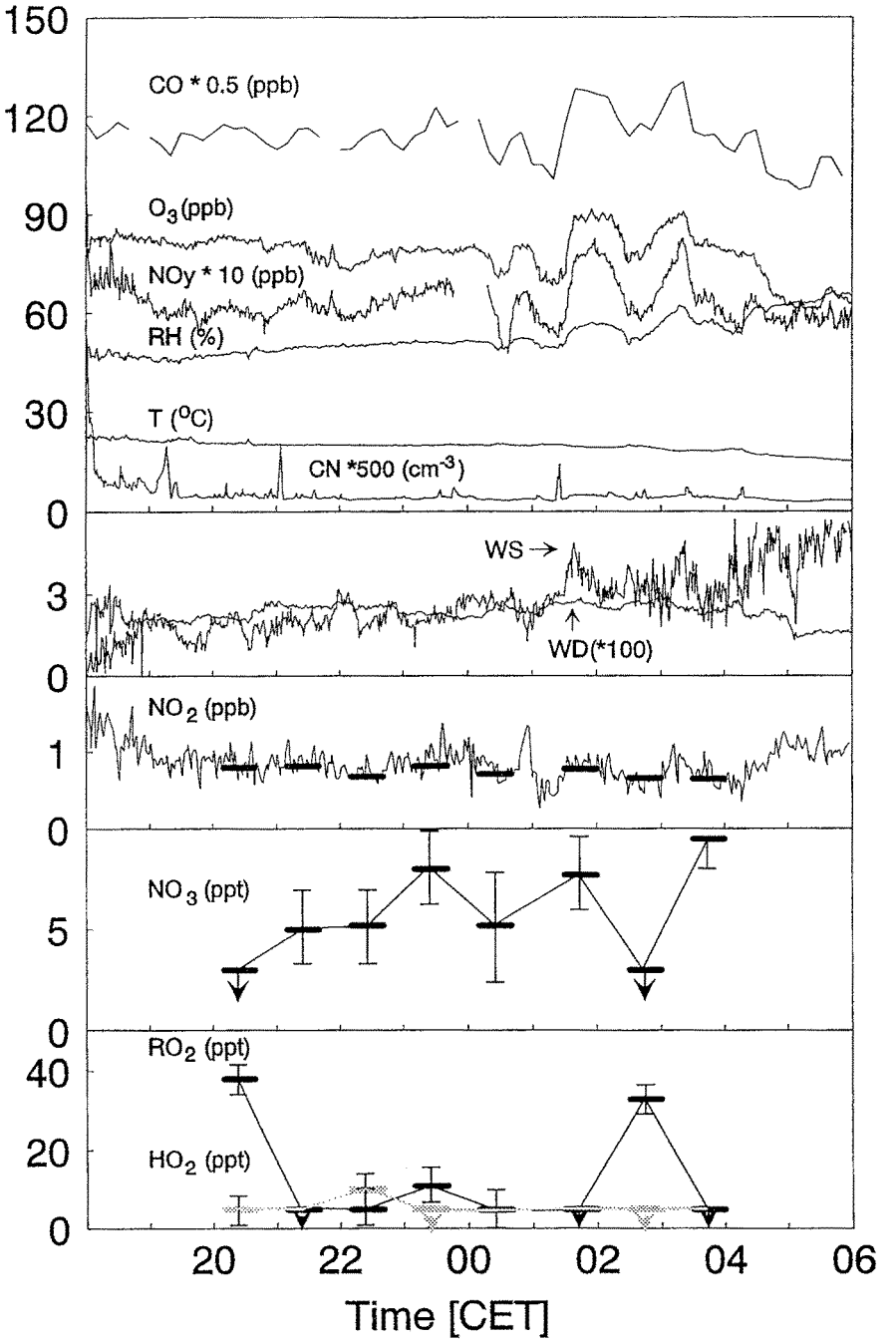

Fig. 4. Night time variation of CO, O_3, NO_y, relative humidity, temperature, aerosol concentration (CN), wind speed (WS), wind direction (WD), NO_2 (chemiluminescence; solid line), NO_2 (MIESR; 30 min averaging), NO_3, HO_2 and $\Sigma(RO_2)$ on 24/25 August 1990, at Schauinsland, Black Forest, 48° N, 8° E, 1150m ASL. The lines shown in the two lower panels represent linear interpolations through the NO_3, HO_2, and $\Sigma(RO_2)$ data ignoring possible variations in the time periods between measured values. The symbols with arrows denote concentrations below the detection limit.

Table I. Night time radical concentrations of HO_2, $\Sigma(RO_2)$, NO_3, effective lifetime of NO_3 and supporting data

Date	Time (CET)	O_3 (ppb)	NO_2 (ppb)	NO_3 (ppt)	$\tau_{eff}(NO_3)$ (sec)	HO_2 (ppt)	$\Sigma(RO_2)$ (ppt)	Temperature (K)	Relative humidity (%)
8-24	20:10–20:40	83	0.80	$\leqslant 3$	$\leqslant 71$	5 ± 4	38 ± 5	294	48
8-24	21:10-21:40	80	0.82	5.0 ± 2	120	$\leqslant 5$	$\leqslant 5$	294	50
8-24	22:10–22:40	78	0.68	5.2 ± 2	156	10 ± 3	5 ± 3	293	50
8-24	23:10–23:40	80	0.82	8.0 ± 2	193	$\leqslant 5$	11 ± 4	293	51
8-25	0:10–0:40	75	0.71	5.2 ± 2	154	$\leqslant 5$	5 ± 4	294	50
8-25	1:30–2:00	90	0.78	7.7 ± 3	176	$\leqslant 5$	$\leqslant 5$	293	56
8-25	2:30–3:00	83	0.66	$\leqslant 3$	$\leqslant 89$	5 ± 3	33 ± 5	293	54
8-25	3:30–4:00	81	0.65	9.5 ± 2	300	$\leqslant 5$	$\leqslant 5$	292	56

Date	Time (CET)	C_2H_2 (ppb)	C_2H_4 (ppb)	C_2H_6 (ppb)	C_3H_6 (ppb)	C_3H_8 (ppb)	1-C_4H_8 (ppb)	¡C_4H_{10} (ppb)	nC_4H_{10} (ppb)	¡C_5H_{12} (ppb)	nC_5H_{12} (ppb)	CH_3CHO (ppb)
8-24	19:29	0.28	0.11	1.30	0.06	0.43	0.02	0.10	0.34	0.27	0.05	0.68
8-24	22:56	0.30	0.16	1.25	0.08	0.44	0.01	0.15	0.42	0.33	0.08	0.77
8-25	2:24	0.30	0.14	1.16	0.04	0.44	0.01	0.14	0.32	0.32	0.05	0.44
8-25	5:50	0.22	0.22	1.10	0.07	0.38	0.01	0.10	0.35	0.27	0.04	0.60

the MIESR samples were collected. The ratio of NO_y to NO_2 was almost 10, which is an indication that photochemically aged air masses were encountered during that night. During the second half of the night, simultaneous variations in CO, O_3, NO_y, NO_2, T, and RH were observed indicating small changes in the air masses arriving at the site. It is noteworthy that both techniques used (e.g. MIESR and photolytic conversion/chemiluminescence) showed a close agreement in the NO_2 data.

The NO_3 levels were rather low, e.g. <10 ppt, given the relatively high temperatures and O_3 concentrations that favoured a fast production from reaction (4). The NO_3 mixing ratio exhibited a more pronounced variation than its longer lived precursors, in particular, during the second half of the night. The concentrations of peroxy radicals varied between almost 40 ppt and values below the detection limit of 5 ppt. As is depicted by the lower panels in Figure 4, most of the peroxy radicals are found in the fraction of alkylperoxy. The HO_2 concentration was most of the time below or at the detection limit, except for one sample collected around 22:30 hr, where HO_2 accounted for 70% of the total peroxy radical concentration. The concentrations of peroxyacyl radicals were always below the detection limit.

An important feature depicted by the data, besides the spectroscopic evidence for the existence of HO_2 radicals at night, was the anticorrelation between NO_3 and RO_2. For the two samples that showed the highest RO_2 concentrations, NO_3 was found to be below its detection limit of 3 ppt.

4. Discussion

During daytime, NO_3 radical concentrations remain well below one ppt, because of rapid photolysis and the fast reaction with NO. After sunset, however, they can reach levels of up to a few hundred ppt (Platt *et al.*, 1980, 1981, 1984; Noxon *et al.*, 1978, 1980, 1983; Brauers *et al.*, 1990).

It was argued that the NO_3 concentration at night approaches a steady state, such that production from reaction (4),

$$NO_2 + O_3 \rightarrow NO_3 + O_2 \tag{4}$$

is matched by losses of both NO_3 and N_2O_5. The latter losses are effective, because thermodynamic equilibrium between NO_2, NO_3, and N_2O_5 (5a, b),

$$NO_3 + NO_2 + M \underset{k_{5b}}{\overset{k_{5a}}{\rightleftharpoons}} N_2O_5 + M \tag{5a, b}$$

is established within less than one minute at temperatures around 20 °C. The steady state NO_3 concentration is given by Equation (6), (Platt *et al.*, 1984), where the denominator is the effective pseudo first-order loss coefficient of NO_3. Under conditions, where the permanent losses of N_2O_5, e.g. $\tau^{-1}_{(N_2O_5)}$, are slow compared to reaction (5b) the term $(1 + k^{-1}_{5b}\,\tau^{-1}_{(N_2O_5)})$ is approximately 1 and the expression for NO_3 can be simplified, e.g. second half of Equation (6). Under the conditions of our measurements $k^{-1}_{5b}\,\tau^{-1}_{(N_2O_5)}$ varied between 0.15 and 1.5. The effective lifetime of

NO_3 can be determined experimentally from the simultaneous concentrations of NO_3, NO_2, and O_3 (Equation 7; Platt *et al.*, 1984),

$$[NO_3] = \frac{[NO_2]\,[O_3]\,k_4}{\dfrac{[NO_2]\,K_5\,\tau^{-1}_{(N_2O_5)}}{1 + k^{-1}_{5b}\,\tau^{-1}_{(N_2O_5)}} + \tau^{-1}_{(NO_3)}}$$

$$\approx \frac{[NO_2]\,[O_3]\,k_4}{[NO_2]\,K_5\,\tau^{-1}_{(N_2O_5)} + \tau^{-1}_{(NO_3)}} \tag{6}$$

$$\tau^{-1}_{\text{eff}} = \frac{[NO_2]\,[O_3]\,k_4}{[NO_3]} \tag{7}$$

$\tau^{-1}_{(NO_3)}$ and $\tau^{-1}_{(N_2O_5)}$ are the first-order loss constants that arise from the different loss processes for N_2O_5 and NO_3, respectively. We have calculated the effective lifetime of NO_3, τ_{eff}, from Equation (7) for each of our measurements (Table I). It ranged from <70 sec for those samples, where only upper limits of the NO_3 concentration were obtained, to a maximum value of 300 sec at the end of the night.

In the following, we shall discuss the potential contributions of the different loss processes to the budget of NO_3 on 24 and 25 August at Schauinsland.

4.1. *Inorganic Losses*

Table II gives the different atmospheric lifetimes of NO_3 that result from the individual homogeneous reactions with inorganic species. Reactions of NO_3 with itself or with NO_2 are by far to slow to be of importance. Johnston *et al.* (1986) had proposed that unimolecular decomposition of NO_3 (8),

$$NO_3 + M \rightarrow NO + O_2 + M \tag{8}$$

could be the missing process needed to explain the atmospheric observations by Noxon *et al.* (1978, 1980). The rate coefficient for this reaction was recently determined by Davidson *et al.*, 1990 in a laboratory study. The resulting lifetime is 450 sec at 293 K, a factor of 1.5 longer than the longest lifetime observed by us. Hence,

Table II. Effective lifetime of NO_3 according to some inorganic reaction

Reaction	Rate constant (cm^3 $molec^{-1}$ sec^{-1})	Species	Concentration (cm^{-3})	τ_{NO_3} (sec)
$NO_3 + NO \rightarrow NO_2 + NO_2$	2.8×10^{-11}	NO	2.23×10^{8}	160
$NO_3 + NO_2 \rightarrow NO + NO_2 + O_2$	5.3×10^{-16}	NO_2	2.23×10^{10}	8×10^{4}
$NO_3 + NO_3 \rightarrow NO_2 + NO_2 + O_2$	3×10^{-16}	NO_3	2.23×10^{8}	1×10^{7}
$NO_3 + M \rightarrow NO + O_2 + M$	1×10^{-22}	M	2.23×10^{19}	450
$N_2O_5 + H_2O \rightarrow HNO_3 + HNO_3$	$<2 \times 10^{-21}$	H_2O	5.00×10^{17}	1000

Reaction rates are for 880 mb and $T = 293$ K, as observed at nighttime in Schauinsland, August, 24/25.

from our measurements alone, we cannot exclude reaction (8) to provide a significant sink for NO_3. Platt *et al.* (1984) on the other hand, observed NO_3 lifetimes in the atmosphere of up to 1 hr (see Figure 5) at an ambient temperature at 291 K. The corresponding lifetime due to (8) would be 507 sec. The results of Platt thus clearly contradict the results of Davidson *et al.*

If the longest atmospheric lifetime observed by Platt *et al.* is interpreted as an atmospheric measurement of the unimolecular decay of NO_3, the rate coefficient k_8 would be at least seven times smaller than that determined in the laboratory.

Therefore, reaction (8) seems unlikely to be of importance for the atmospheric NO_3 budget at Schauinsland. As was discussed by Heikes and Thomson (1983), and by Russel *et al.* (1985, 1986), in their interpretation of the data measured by Platt *et al.* (1980, 1984), the greatest uncertainty in the nocturnal NO_3 balance arises from reaction (9).

$$NO_3 + NO \rightarrow NO_2 + NO_2. \tag{9}$$

The chemiluminescence detector used by us for NO measurements at Schauinsland has a detection limit of about 20 ppt for an integration time of 30 min, mostly because of the potential existence of a spurious signal, the so-called fake NO. Averaged over the whole sampling period the measured NO corresponds to a mixing ratio of 7 ± 10 ppt. Although this spurious signal might, at least partially, be caused by an instrumental artifact, we cannot exclude the presence of NO at mixing ratios of up to 20 ppt. The resulting lower limit on the NO_3 lifetime is 80 sec, which is very close to the maximum lifetime calculated for those samples, where NO_3 was below our detection limit. From the NO measurements alone, we thus cannot exclude reaction (9) to be the predominating NO_3 loss. We shall address this point below in the context of model simulations that we have performed.

The homogeneous reaction of NO_3 with H_2O is endothermic. For the respective reaction of N_2O_5,

$$N_2O_5 + H_2O \rightarrow HNO_3 + HNO_3 \tag{10}$$

a relatively high upper limit of $k_{10} < 2 \times 10^{-21}$ cm^3 molec^{-1} sec^{-1} is still recommended (Atkinson *et al.*, 1989), although Sverdrup *et al.* (1987) have determined a much lower value of $k_{10} \leqslant 3 \times 10^{-22}$ cm^3 molec^{-1} sec^{-1}, which is in much better agreement with the atmospheric observations (Platt *et al.*, 1984). If the latter value is adopted, a corresponding NO_3 lifetime around 10^4 sec is derived. Even with the upper limit recommended by Atkinson *et al.* (1989), the homogeneous reaction of N_2O_5 with H_2O would be unimportant for the budget of NO_3 under the conditions of our measurements.

4.2. *Heterogeneous Losses*

Heterogeneous losses of N_2O_5 and NO_3 on liquid water surfaces of aerosol particles can provide an efficient sink for atmospheric NO_3. The rate of removal

depends on the surface area and size of the aerosols, the sticking coefficient of the substance at the surface, the solubility of the compound to be absorbed, and the availability of chemicals in the solution, that serve to irreversibly remove the dissolved trace gas. The sticking coefficients of both NO_3 and N_2O_5 at aqueous surfaces are reasonably large, e.g. $\gamma(NO_3) > 2.5 \times 10^{-3}$ (Thomas *et al.*, 1989) and $\gamma(N_2O_5) > 10^{-2}$ (Mozurkewich and Calvert, 1988; Kirchner *et al.*, 1990). The solubility of N_2O_5 is, because of its fast hydrolysis, generally assumed to be infinite. The Henry coefficient of NO_3 has been determined experimentally to $K_H(NO_3) = (1.8 \pm 1.5)$ mole l^{-1} atm^{-1} (Thomas, 1992). Dissolved NO_3 radicals are known to undergo fast reactions with HSO_3^- and Cl^- ions (Neta and Huie, 1986; Herrmann *et al.*, 1992), which can greatly enhance its heterogeneous removal despite its relatively low solubility. As stated above, N_2O_5 and NO_3 concentration are calculated to be about equal. Hence, heterogeneous losses of either species would have had a similar impact on the NO_3 budget at Schauinsland.

An important finding of Platt *et al.* (1984) was that the atmospheric lifetime of NO_3 decreased sharply under conditions where the relative humidity increased above 45%. They attributed this to an increasing efficiency of the heterogeneous removal processes, because aerosols are known to grow considerably by incorporation of water, when the relative humidity exceeds the deliquescence point, which for several salts is in the range of 50% (Mozurkewich and Calvert, 1988 and references therein). In Figure 5, we have reproduced the graph of Platt *et al.* (1984) and included the NO_3 lifetimes calculated from our measurements. They are consistent with the lifetimes of <10 min that were observed by Platt *et al.* at humidities around

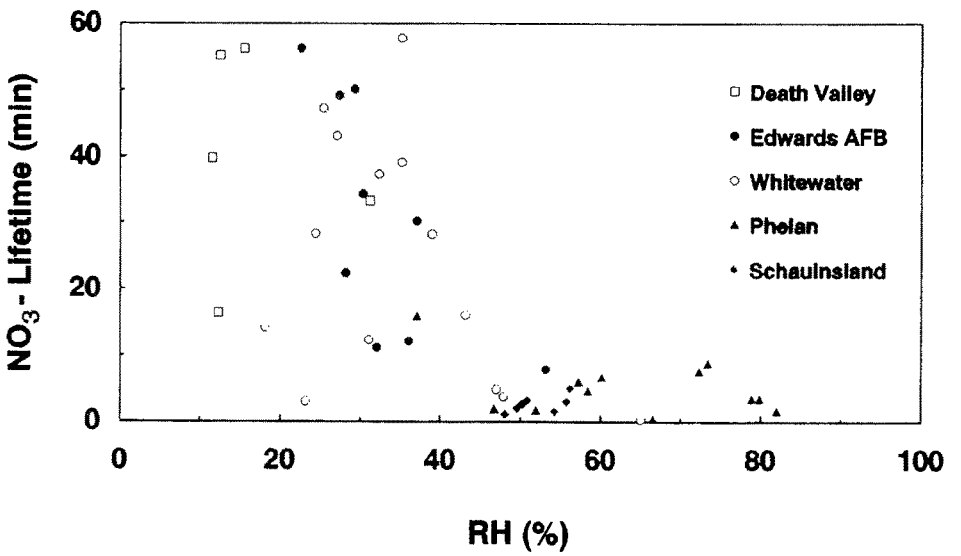

Fig. 5. Lifetime of NO_3, $\tau(NO_3)$, observed at a variety of locations around the Mojave Desert (Platt *et al.*, 1984) and at Schauinsland (this work) as a function of relative humidity.

and above 50%. For this reason, we cannot exclude that the short lifetimes of NO_3 observed by us were mainly caused by heterogeneous losses, although the particle concentrations at Schauinsland were quite low during that night, namely around 2500 cm^{-3} (see Figure 4).

There are several arguments that point against heterogeneous losses as the only important sink of NO_3 during that night. Firstly, the NO_3 concentration showed a strong variation, whereas the aerosol concentration was rather constant, except for a few short spikes. Secondly, the continuous increase in relative humidity during the night was not reflected in a corresponding decrease in the NO_3 lifetime. The highest relative humidity was observed during the time when the last sample was collected. In this sample we found the highest NO_3 concentration (9.5 ppt) and no peroxy radicals (<5 ppt). Therefore, we can use this sample to calculate an upper limit of the effective pseudo-first-order rate coefficient for heterogeneous removal of $<3 \times 10^{-3}$ sec^{-1}.

4.3. *Organic Losses*

The most important observation was the presence of significant amounts of peroxy radicals and the pronounced anticorrelation between RO_2 and NO_3 concentrations. This finding strongly suggests the importance of reactions with organic molecules. In order to explore the role of these reactions for the nocturnal radical budget, we have simulated our observations with a chemical box model. The reaction scheme included homogeneous reactions with inorganic and organic species as well as heterogeneous losses of both NO_3 and N_2O_5 (for the details, see the appendix). Temperature, pressure and the concentrations of NO_2, O_3, H_2O_2, CO, and C_2—C_5 hydrocarbons were fixed to the measured values and CH_4 was fixed at 1.7 ppm. Since only four hydrocarbon measurements fell into the time interval, where the MIESR samples were collected, the respective concentrations at each sampling time were calculated by linear interpolation, which is justified because of the fairly constant values observed for all of the long-lived trace gases during the night.

The heterogeneous loss rate was adjusted such that the model correctly reproduced the NO_3 concentration of the last sample (3×10^{-3} sec^{-1}), for which the longest lifetime was determined experimentally (Equation (7)). The same heterogeneous loss rate was then used in the model simulations of the other seven samples.

The results of the base run are compared with the NO_3 and RO_2 measurements in Figure 6. It is obvious that the measured anthropogenic hydrocarbons are not sufficient to explain the observed RO_2 concentrations. In particular, the RO_2 concentrations around 40 ppt found in samples 1 and 7 are underestimated in the model by more than an order of magnitude. Also, the model significantly overestimated the NO_3 concentrations in these samples. In Table III we have listed the pseudo-first-order rate coefficients that are calculated in the model for the different reactions with organic and inorganic species. The most important sink for NO_3 is

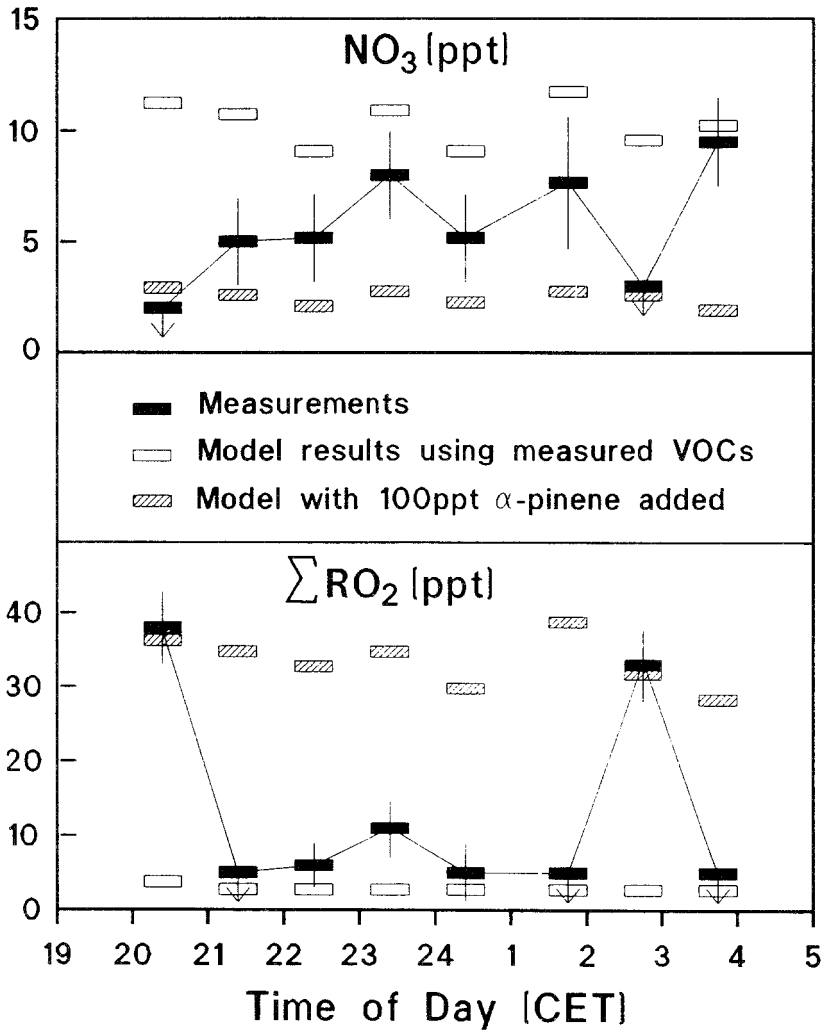

Fig. 6. Nighttime variation of NO_3 radicals and sum of alkyl peroxy radicals measured (solid line; 30 min averages and standard deviations) at Schauinsland, 24/25 August 1990, in comparison with the box model calculations for two examples: Empty rectangles represent the calculations with only measured hydrocarbons included. Dashed rectangles represent calculations including 100 ppt of α-pinene. The lines represent a linear interpolation curve through the measured and simulated $\Sigma(RO_2)$ data ignoring possible variations in the time periods between the rectangles. The symbols with arrows denotes concentrations below the detection limit.

the above-defined $\tau_{het}^{-1} = 3 \times 10^{-3}$ sec^{-1} which accounts for approximately 90% of the NO_3 losses. In addition, significant losses arise from reaction with H_2O_2, because of the fairly high concentrations (up to 4 ppb) observed during that night. Reactions with hydrocarbons are not of importance for the NO_3 budget. In total, they provide a first-order loss coefficient of 1.2×10^{-4} sec^{-1}. The most important individual organic species are acetaldehyde and methane.

Table III. Loss rate of NO_3 with organic and inorganic species

R		CO	H_2O_2	CH_4	C_2H_4	C_3H_6	1-C_4H_8	nC_4H_{10}	nC_5H_{12}	Isoprene	CH_2O	CH_3CHO
Mixing ratio	[ppb]	200	4	1700	0.16	0.08	0.02	0.34	0.08	0.005	1	0.8
k_{NO_3}	[cm^3 molecule^{-1} s^{-1}]	4×10^{-19}	$<2\times10^{-15}$	$<1\times10^{-18}$	2×10^{-16}	9.5×10^{-15}	1.6×10^{-14}	3.8×10^{-17}	4×10^{-17}	5.5×10^{-13}	5.8×10^{-16}	2.5×10^{-15}
$\tau^{-1}_{NO_3}$	[sec^{-1}]	1.8×10^{-6}	1.8×10^{-4}	3.8×10^{-5}	7.4×10^{-7}	1.8×10^{-5}	6×10^{-6}	3×10^{-7}	7×10^{-8}	6×10^{-5}	1.3×10^{-5}	4.6×10^{-5}

Reaction rates are for 880mb and T = 293 K, as observed at nighttime in Schauinsland, August, 24/25.

Although the analysis of hydrocarbons $>C_5$ has not been finalized, it is clear from the chromatograms that their concentrations decreased substantially with chain-length. This is in accordance with the large NO_y/NO_x ratio found in this air-masses indicating that the short-lived species have already been depleted. Hence, the higher alkanes cannot have contributed much to NO_3 removal nor to RO_2 production because of their slow reaction with NO_3. Formaldehyde concentrations were set equal to 1 ppb, a value representative of measurements performed under similar conditions during a field campaign in 1989 (Klemp, 1992). Even the maximum concentration of 5 ppb that was observed in 1989 during a photochemical episode, when polluted air from the Rhine valley was encountered, would not make HCHO to a significant sink for NO_3. Likewise, the measured alkenes do have an insignificant impact on the radical budget of that night. They provide a first-order NO_3 loss of only 2.5×10^{-5} sec^{-1}. Since higher alkenes than 1-butene were not observed and because the reactions of NO_3 with aromatics are rather slow, we conclude that the anthropogenic hydrocarbons present in the aged air masses traced by our measurements did not have a large impact on the NO_3 budget. In particular, their concentrations were insufficient to explain the observed peroxy radical concentrations. The same holds for isoprene, the only natural hydrocarbon that was measured at Schauinsland. Its concentration was <5 ppt and its contribution to the NO_3 losses was only 6×10^{-5} sec^{-1}.

4.4. *The Potential Role of Monoterpenes*

Monoterpenes are known to react extremely rapidly with NO_3 (cf. table 4; Atkinson, 1990 and references therein). They have been found to be present over forested areas at concentrations up to several hundred ppt. The major compounds identified were α- and β-pinene, camphene, d-limonene, Δ^3-carene, α- and γ-terpinene (Arnts *et al.*, 1982; Yokouchi *et al.*, 1983; Isidorov *et al.*, 1985; Roberts *et al.*, 1985; Anastasi *et al.*, 1991). They are thus likely candidates for explaining both the low NO_3 concentrations and the high RO_2 concentrations found in sample Nos. 1 and 7. Measurements of terpenes had not been made at Schauinsland during this campaign. We investigated their potential impact by including α-pinene in the model as a surrogate and have than used the model to find the concentration of α-pinene necessary to explain both, the NO_3 and RO_2 concentrations found in samples 1 and 7. The results are also shown in Figure 6. It is seen that about 100 ppt α-pinene are required to explain the highest RO_2 concentrations observed. At the same time, the model predicted correctly the low NO_3 concentrations in these samples. In Table IV, the production rates for RO_2 radicals from the different processes are listed. They were calculated for the assumption of an RO_2 yield of 100% and for the yields estimated for ozonolysis for the different olefins (Atkinson and Lloyd, 1984), respectively. RO_2 radicals are predominantly due to the reaction of α-pinene with NO_3. Clearly, the other samples require only 10–20% of the terpene concentrations to explain the RO_2 and NO_3 concentrations. The strong fluctua-

Table IV. Comparison of rate constant and production rates of peroxy radicals for selected hydrocarbons in the presence of 80 ppb of O_3 and 10 ppt of NO_3 radicals

Species	Mixing ratio (ppt)	Rate constant (k_{O_3}) ($cm^3 \cdot molec^{-1} sec^{-1}$)	Production rate (molec cm^{-3} sec^{-1})	Rate constant (k_{NO_3}) ($cm^3 \cdot molec^{-1} sec^{-1}$)	Production rate (molec cm^{-3} sec^{-1})
C_2H_4	160	1.5×10^{-18}	1×10^{3} [a]	1.8×10^{-16}	1.4×10^{2}
C_3H_6	80	1×10^{-17}	1.3×10^{4} [a]	9.4×10^{-15}	3.7×10^{3}
1-C_4H_8	20	1×10^{-17}	3.2×10^{3} [a]	1.3×10^{-14}	1.3×10^{3}
Isoprene	5	1.4×10^{-17}	2.8×10^{3} [b]	5.5×10^{-13}	1.5×10^{4}
α-Pinene	100	8×10^{-17}	3.2×10^{b} [b]	5.7×10^{-12}	2.8×10^{6}
α-Terpinene	4	8.8×10^{-14}	1.4×10^{7} [b]	1.8×10^{-10}	3.6×10^{6}

Reaction rates are for 880 mb and $T = 293$ K, as observed at nighttime in Schauinsland, 24/25 August.

[a] Production rate includes the fraction of peroxy radical formation (Atkinson and Lloyd, 1984).

[b] Under assumption of 100% yield of peroxy radicals formed.

tions of radical species are in contrast to the small variability of the longer-lived trace gases. They are most likely caused by small-scale turbulence changing the composition of the air mass with respect to the natural hydrocarbons and, possibly, NO (see below).

The yield of peroxy radicals from the ozonolysis of α-pinene is not accurately known. However, even under the assumption that all the Criegee biradicals initially formed would lead to peroxy radical formation, only 10% of the total RO_2 production would come from the reaction with O_3 and 90% from that with NO_3. The measured alkenes ethene, propene, 1-butene, and isoprene account for less than 3% of the RO_2 radicals.

In another simulation we replaced α-pinene by one of the most reactive natural hydrocarbons, namely α-terpinene. The respective concentration required to explain the observed NO_3 and RO_2 concentrations was only 4 ppt.

These simulations demonstrate that the short lifetimes of NO_3 for samples 1 and 7 of less than 70 sec and the simultaneously observed large concentrations of peroxy radicals strongly suggest the presence of monoterpenes at individual concentrations in the range of 1–100 ppt. Such concentrations are not inconceivable in view of the existing measurements, in particular at the high temperature of that night.

A few measurements of monoterpenes were made at Schauinsland during a field campaign in 1984 (Platt *et al.*, 1988). The maximum concentrations then found for the monoterpenes α-pinene (80 ppt), terpinene (52 ppt), and limonene (57 ppt) would be sufficient to explain the RO_2 concentrations measured by us. It is emphasized that the need for monoterpenes comes exclusively from the RO_2 measurements, whereas the short lifetimes of NO_3 alone could be explained on the basis of other processes, for example heterogeneous losses or reaction with NO.

Another important information in our measurements is the presence of HO_2

radicals at night. HO_2 was positively identified in three samples, although only in one sample (No. 3, 10 ppt HO_2) was its concentration significantly above the detection limit (see Figure 2). HO_2 radicals are produced in the metabolism of RO_2 radicals via reaction of alkoxy radicals with oxygen. The most important initial reactions are those of RO_2 with NO and NO_3, whereas the RO_2—RO_2 permutation reactions are too slow in order to produce large amounts of HO_2 (see Appendix). Of course, NO and NO_3 also serve to remove HO_2. However, at the high CO concentrations observed at Schauinsland (250 ppb), recycling of the HO_2 radicals from the OH thus formed is rather efficient.

Our model simulations show that NO_3 concentrations are too small to provide a fast enough production of HO_2 under the conditions of our measurements, as is exhibited by Figure 6. We have thus investigated the potential influence of higher NO concentrations on the budgets of NO_3, RO_2, and HO_2 radicals. For this purpose, we used the model with α-pinene (100 ppt) and increased the NO concentration to 5 and 10 ppt, respectively. The most important implication is that a steady-state NO concentration of 5 ppt implies a flux of NO into the box of about 3×10^6 molec cm^{-3} sec^{-1}, whereas the removal rate for NO_2 due to reaction with O_3 is only 0.8×10^6 molec cm^{-3} sec^{-1} at the measured concentrations. In steady state, the coexistence of 5 ppt of NO, 80 ppb of O_3 and 0.7 ppb NO_2 implies an additional NO_2 sink of 2.2×10^6 molec cm^{-3} sec^{-1}. The required removal process could be provided either by dry deposition or by dispersion.

In order to calculate the corresponding flux, the height of the nocturnal near-surface inversion would have to be known. The balloon soundings we have made during the campaign showed such inversions to be present 150 m above the ground. The lower bound for such an inversion would be the height, where our measurements were made, e.g. 15 m. The corresponding deposition velocity at an NO_2 concentration of 0.65 ppb would be 0.25 cm sec^{-1}, which is in agreement with values determined by field experiments (Hanson and Lindberg, 1991). Of course, at least the same deposition velocity would have to be included for NO_3 and N_2O_5. It would correspond to an effective lifetime for NO_3 of 3000 sec. Even a four times faster deposition velocity of 1 cm sec^{-1}, which is more likely for compounds that are highly soluble or undergo chemical reactions (Hanson and Lindberg, 1991, and references therein), does not have a substantial effect on the NO_3 budget.

The NO flux from the surface required to balance its removal by O_3, again assuming a scale-height of 15 m, is about 5×10^9 molec cm^{-2} sec^{-1}, which is again not inconceivable in the light of the existing measurements of soil emissions (Slemr and Seiler, 1984; Anderson and Levine, 1987; Parish *et al.*, 1987; Williams *et al.*, 1987, 1988). Assuming a larger scale-height would increase both, the required flux of NO and the deposition velocity of NO_2. Besides dry deposition, the required NO_2 loss could also be provided by vertical exchange. Since we have no information on the vertical gradient of either species, we cannot distinguish between these two processes.

The concentration of α-pinene required to produce RO_2 concentrations of 40

ppt in the presence of 5 ppt of NO is 0.6 ppb, which is very close to the nocturnal concentrations of terpenes measured at Niwot Ridge (Roberts *et al.*, 1985) or daytime concentrations measured at Schauinsland (Platt *et al.*, 1988). The corresponding flux of monoterpenes into a 15 m box required to balance the losses by reaction with NO_3 and O_3 is about 4×10^9 molec cm^{-2} sec^{-1}. Anastasi *et al.* (1990) have calculated terpene emission for the South of the U.K. which are, on the average, 2×10^{11} molec cm^{-2} sec^{-1}. At a temperature of 20 °C, the flux could be even larger (Lamb *et al.*, 1987; Yokouchi *et al.*, 1983). Hence, the concentrations of both NO and monoterpenes required to explain the observed concentrations of RO_2 and HO_2 radicals are consistent with the existing information on the respective emissions in forested areas.

Recently Atkinson *et al.* (1992) reported the formation yields of OH radicals in the ozonolysis of a series of terpenes. We have performed additional model simulations with α-pinene, including this process. The results indicate that the direct production of OH and, consequently HO_2, in the reaction of O_3 with α-pinene, is not sufficient to explain the measured HO_2 and RO_2 concentrations in the absence of NO. However, the required NO concentration is reduced, by ~30%.

5. Conclusions

We have presented experimental data on the near-surface concentrations of NO_3 and peroxy radicals at night in a forested area, together with measurements of the concentrations of CO, O_3, NO_x, NO_y, and hydrocarbons as well as meteorological parameters.

The chemical budgets of both radical species can be understood on the basis of box model simulations, if emissions of monoterpenes are included. The measured HO_2 levels could only be explained by the model, when NO concentrations around 5 ppt were assumed to be present. The fluxes of NO and monoterpenes required in the model to describe the observations, are consistent with existing measurements. From our analysis it is clear, that two samples (No. 1 and 7) require the recent input of monoterpenes, whereas sample No. 3 suggest that the RO_2 radicals have already been converted to HO_2, which is still present in the air parcel, most likely due to recycling within the HO_x family.

The major losses for HO_x in the model are reactions of OH with NO_2 and hydrocarbons, which than leads back to RO_2 formation. The presence of HO_2 radicals in concentrations up to 10 ppt also implies the presence of hydroxyl radicals at night in concentrations of up to 10^5 molec cm^{-3}, as was recently suggested by Platt *et al.* (1990).

It is clear that not all the observed features can be understood with the simple steady-state approach used in this study. The strong variations observed in NO_3, RO_2, and HO_2 concentrations are in contrast to the almost constant values of the longer-lived species. This behaviour clearly indicates the influence of small-scale turbulence and interactions with the surface or the canopy.

A full explanation would require statistical treatment of the surface layer in combination with additional measurements of the natural hydrocarbons and additional micro-meteorological parameters to quantify the turbulent exchange.

Acknowledgements

The authors are grateful to R. Graul and the group of the UBA monitoring station on the Schauinsland for their hospitality and cooperation during the field campaign. We would also like to thank F. Flocke, H. Fark, R. Bauer, and F. Rohrer for valuable contributions. Part of this project was supported by BMFT in the framework of the EUROTRAC subproject TOR, under grant No. 07 Eu 723.

Appendix

Reaction processes and their rate parameters used in the present simulations

No.	Reaction			Rate constant[a]
R1	$NO_2 + O_3$	$\rightarrow$	$NO_3 + O_2$	$k = 2.8 \times 10^{-17}$
R2	$NO_3 + NO_2$	$\overset{M}{\leftrightarrow}$	N_2O_5	$K = 5.17 \times 10^{-11}$
R3	$NO_3 + NO_3$	$\rightarrow$	$NO_2 + NO_2 + O_2$	$k = 2 \times 10^{-16}$
R4	NO_3	$\overset{M}{\rightarrow}$	$NO + O_2$	$k = 2.3 \times 10^{-3}$
R5	$NO_3 + NO$	$\rightarrow$	$NO_2 + NO_2$	$k = 2 \times 10^{-11}$
R6	$NO_3 + NO_2$	$\rightarrow$	$NO_2 + NO + O_2$	$k = 5.7 \times 10^{-16}$
R7	$NO_3 + CO$	$\rightarrow$	$CO_2 + O_2$	$k < 4 \times 10^{-19}$
R8	$NO_3 + CH_4$	$\overset{O_2}{\rightarrow}$	$CH_3O_2 + HNO_3$	$k < 4 \times 10^{-19}$
R9	$NO_3 + CH_2O$	$\overset{O_2}{\rightarrow}$	$HO_2 + HNO_3 + CO$	$k = 5.8 \times 10^{-16}$
R10	$NO_3 + CH_3CHO$	$\overset{O_2}{\rightarrow}$	$CH_3COO_2 + HNO_3$	$k = 2.1 \times 10^{-15}$
R11	$NO_3 + H_2O_2$	$\rightarrow$	$HO_2 + HNO_3$	$k < 2 \times 10^{-15}$
R12	$NO_3 + C_2H_4$	$\overset{O_2}{\rightarrow}$	$C_2H_4O_3NO_2$	$k = 2 \times 10^{-16}$
R13	$NO_3 + C_3H_6$	$\overset{O_2}{\rightarrow}$	$C_3H_6O_3NO_2$	$k = 9.4 \times 10^{-15}$
R14	$NO_3 + C_4H_8$	$\overset{O_2}{\rightarrow}$	$C_4H_8O_3NO_2$	$k = 1.3 \times 10^{-14}$
R15	$NO_3 + HO_2$	$\rightarrow$	$OH + NO_2 + O_2$	$k = 3.6 \times 10^{-12}$
R16	$NO_3 + HO_2$	$\rightarrow$	$HNO_3 + O_2$	$k = 9.2 \times 10^{-13}$
R17	$NO_3 + CH_3O_2$	$\overset{O_2}{\rightarrow}$	$HO_2 + CH_2O + NO_2$	$k = 2.3 \times 10^{-12}$
R18	$NO_3 + C_2H_4O_3NO_2$	$\rightarrow$	products	$k = 2.6 \times 10^{-13}$
R19	$NO_3 + C_3H_6O_3NO_2$	$\rightarrow$	products	$k = 2.6 \times 10^{-13}$
R20	$NO_3 + C_4H_8O_3NO_2$	$\rightarrow$	products	$k = 2.6 \times 10^{-13}$
R21	NO_3 + Particles	$\rightarrow$	products	$k = 1.3 \times 10^{-3}$
R22	N_2O_5 + Particles	$\rightarrow$	products	$k = 1.3 \times 10^{-3}$
R23	$N_2O_5 + H_2O$	$\rightarrow$	$2 \cdot HONO_2$	$k < 3 \times 10^{-22}$
R24	$O_3 + NO$	$\rightarrow$	$O_2 + NO_2$	$k = 1.7 \times 10^{-14}$
R25	$O_3 + C_2H_4$	$\rightarrow$	$CH_2O + 0.4 \cdot CH_2O_2$	$k = 1.7 \times 10^{-18}$
		$\rightarrow$	$0.4 \cdot CO + 0.1 \cdot HO_2$	
R26	$O_3 + C_3H_6$	$\rightarrow$	$0.5 \cdot CH_2O + 0.5 \cdot CH_3CHO$	$k = 1.1 \times 10^{-17}$
		$\rightarrow$	$0.2 \cdot CH_2O_2 + 0.2 \cdot CH_3CHO_2$	
		$\rightarrow$	$0.3 \cdot CO + 0.2 \cdot HO_2$	
		$\rightarrow$	$0.1 \cdot OH + 0.2 \cdot CH_3O_2$	

[a] Reaction rates are for 880 mb and $T = 293$ K, as observed at nighttime in Schauinsland, 24/25 August.

No.	Reaction			Rate constant[a]
R27	$O_3 + C_4H_8$	$\rightarrow$	$0.5 \cdot CH_2O + 0.5 \cdot CH_3CHO$	$k = 1.1 \times 10^{-17}$
		$\rightarrow$	$0.2 \cdot CH_2O_2 + 0.2 \cdot C_2H_5CHO_2$	
		$\rightarrow$	$0.3 \cdot CO + 0.3 \cdot CO_2 + 0.2 \cdot HO_2$	
		$\rightarrow$	$0.1 \cdot OH + 0.2 \cdot C_2H_5O_2$	
R28	$O_3 + HO_2$	$\rightarrow$	$OH + 2 \cdot O_2$	$k = 6.5 \times 10^{-14}$
R29	$O_3 + OH$	$\rightarrow$	$HO_2 + O_2$	$k = 2 \times 10^{-15}$
R30	$OH + NO_2$	$\xrightarrow{M}$	HNO_3	$k = 1.2 \times 10^{-11}$
R31	$OH + CO$	$\xrightarrow{O_2}$	$HO_2 + CO_2$	$k = 1.5 \times 10^{-13} \times (1 + 0.6\ p(atm))$
R32	$OH + HO_2$	$\rightarrow$	$H_2O + O_2$	$k = (7 + 4\ p(atm)) \times 10^{-11}$
R33	$OH + H_2O_2$	$\rightarrow$	$HO_2 + H_2O$	$k = 1.6 \times 10^{-12}$
R34	$OH + CH_4$	$\xrightarrow{O_2}$	$CH_3O_2 + H_2O$	$k = 7 \times 10^{-15}$
R35	$OH + C_2H_4$	$\xrightarrow{O_2}$	$C_2H_4OHO_2$	$k = 8.2 \times 10^{-12}$
R36	$OH + C_3H_6$	$\xrightarrow{O_2}$	$C_3H_6OHO_2$	$k = 2.6 \times 10^{-11}$
R37	$OH + C_4H_8$	$\xrightarrow{O_2}$	$C_4H_8OHO_2$	$k = 3.4 \times 10^{-11}$
R38	$OH + CH_2O$	$\xrightarrow{O_2}$	$H_2O + HO_2 + CO$	$k = 1 \times 10^{-11}$
R39	$OH + CH_3CHO$	$\xrightarrow{O_2}$	$CH_3COO_2 + H_2O$	$k = 2.1 \times 10^{-15}$
R40	$HO_2 + HO_2$	$\rightarrow$	$H_2O_2 + O_2$	$k = 1.6 \times 10^{-11}$
R41	$HO_2 + NO_2$	$\overset{M}{\leftrightarrow}$	HO_2NO_2	$K = 3 \times 10^{-11}$
R42	$HO_2 + NO$	$\rightarrow$	$OH + NO_2$	$k = 8.4 \times 10^{-12}$
R43	$HO_2 + CH_3O_2$	$\rightarrow$	$CH_3OOH + O_2$	$k = 5 \times 10^{-12}$
R44	$HO_2 + CH_3COO_2$	$\rightarrow$	$CH_3COOH + O_2$	$k = 5 \times 10^{-12}$
R45	$CH_3O_2 + NO$	$\xrightarrow{O_2}$	$CH_2O + HO_2 + NO_2$	$k = 7.8 \times 10^{-12}$
R46	$CH_3O_2 + CH_3O_2$	$\rightarrow$	$2 \cdot CH_2O + 2 \cdot HO_2$	$k = 1.4 \times 10^{-13}$
R47	$CH_3O_2 + CH_3O_2$	$\rightarrow$	$CH_2O + CH_3OH + O_2$	$k = 2.5 \times 10^{-13}$
R48	$CH_3COO_2 + NO_2$	$\overset{M}{\leftrightarrow}$	PAN	$K = 2.9 \times 10^{-8}$
R49	$CH_3COO_2 + NO$	$\xrightarrow{O_2}$	$CH_3O_2 + NO_2 + CO_2$	$k = 2.1 \times 10^{-11}$
R50	$C_2H_4O_3NO_2 + NO$	$\xrightarrow{O_2}$	products	$k = 7.8 \times 10^{-12}$
R51	$C_3H_6O_3NO_2 + NO$	$\xrightarrow{O_2}$	products	$k = 7.8 \times 10^{-12}$
R52	$C_4H_8O_3NO_2 + NO$	$\xrightarrow{O_2}$	products	$k = 7.8 \times 10^{-12}$
R53	$CH_2O_2 + NO$	$\rightarrow$	$CH_2O + NO_2$	$k = 7 \times 10^{-12}$
R54	$CH_2O_2 + NO_2$	$\rightarrow$	$CH_2O + NO_3$	$k = 7 \times 10^{-13}$
R55	$CH_2O_2 + H_2O$	$\rightarrow$	$CH_2O + H_2O_2$	$k = 3.3 \times 10^{-18}$
R56	$CH_3CHO_2 + NO$	$\rightarrow$	$CH_3CHO + NO_2$	$k = 7 \times 10^{-12}$
R57	$CH_3CHO_2 + NO_2$	$\rightarrow$	$CH_3CHO + NO_3$	$k = 7 \times 10^{-13}$
R58	$CH_3CHO_2 + H_2O$	$\rightarrow$	$CH_3CHO + H_2O_2$	$k = 3.3 \times 10^{-18}$
R59	$C_2H_5CHO_2 + NO$	$\rightarrow$	$C_2H_5CHO + NO_2$	$k = 7 \times 10^{-12}$
R60	$C_2H_5CHO_2 + NO_2$	$\rightarrow$	$C_2H_5CHO_2 + NO_3$	$k = 7 \times 10^{-13}$
R61	$C_2H_5CHO_2 + H_2O$	$\rightarrow$	$C_2H_5CHO_2 + H_2O_2$	$k = 3.3 \times 10^{-18}$
R62	$RH + NO_3$	$\xrightarrow{O_2}$	RHO_3NO_2	$k = 5 \times 10^{-12}$
R63	$RHO_3NO_2 + NO$	$\xrightarrow{O_2}$	$NO_3RO + NO_2 + HO_2$	$k = 7 \times 10^{-12}$
R64	$RH + OH$	$\xrightarrow{O_2}$	$RHOHO_2$	$k = 6 \times 10^{-11}$
R65	$RHOHO_2 + NO$	$\xrightarrow{O_2}$	$ROHO + NO_2 + HO_2$	$k = 7 \times 10^{-12}$

[a] Reaction rates are for 880 mb and $T = 293$ K, as observed at nighttime in Schauinsland, 24/25 August.

References

Anastasi, C., Hopkinson, L., and Simson, V. J., 1991, Natural hydrocarbon emission in the United Kingdom, *Atmos. Environ.* **25**, 1403–1408.

Anderson, I. C. and Levine, J. S., 1987, Simultaneous field measurements of biogenic emissions of nitric oxide and nitrous oxide, *J. Geophys. Res.* **92**, 965–976.

Arnts, R. R., Petersen, W. B., Seila, R. L., and Gay, B. W. Jr., 1982, Estimates of α-pinene emissions from a loblolly pine forest using an atmospheric diffusion model, *Atmos. Environ.* **16**, 2127–2137.

Atkinson, R. and Lloyd, A. C., 1984, Evaluation of kinetic and mechanistic data for modeling of photochemical smog, *J. Phys. Chem. Ref. Data* **13**, 315–444.

Atkinson, R., Baulch, D. L., Cox, R. A., Hampson, R. F. Jr., Kerr, J. A., and Troe, J., 1989, Evaluated kinetic and photochemical data for atmospheric chemistry: Supplement III, *J. Phys. Chem. Ref. Data* **18**, 881–1097.

Atkinson, R., 1991, Kinetics and mechanisms of the gas-phase reactions of the NO_3 radical with organic compounds, *J. Phys. Chem. Ref. Data* **20**, 449–507.

Atkinson, R., Aschmann, S. M., Arey, J., and Shorees, B., 1992, Formation of OH radicals in the gas phase reactions of O_3 with a series of terpenes, *J. Geophys. Res.* **97**, 6065–6073.

Brauers, T., Dorn, H.-P., and Platt, U., 1990, Spectroscopic measurements of NO_2, O_3, SO_2, IO and NO_3 in maritime air, in G. Restelli and G. Angeletti (eds.), *Physico-Chemical Behaviour of Atmospheric Pollutants*, Proc. 5th European Symposium, Varesse, Italia, Kluwer Academic Publishers, Dordrecht, pp. 237–242.

Cantrell, C. A., Stockwell, W. R., Anderson, L. G., Busarow, K. L., Perner, D., Schmeltekopf, A., Calvert, C. A., and Johnston, H. S., 1985, Kinetic study of the NO_3—CH_2O reaction and its possible role in the night-time tropospheric chemistry, *J. Phys. Chem.* **89**, 139–146.

Crowley, J. N., Burrows, J. P., Moortgat, G. K., Poulet, G., and LeBrass, G., 1990a, Room temperature rate coefficient for the reaction between CH_3O_2 and NO_3, *Int. J. Chem. Kin.* **22**, 673–681.

Crowley, J. N., Bauer, D., Burrows, J. P., Moortgat, G. K., Poulet, G., and LeBrass, G., 1990b, Laboratory studies of the gas phase reaction between NO_3 and simple peroxy radicals, *XIth Int. Symp. Gas Kinetics*, Assisi, Italy, 2–7 September.

Davidson, J. A., Cantrell, C. A., Shetter, R. E., McDaniel, A. H., and Calvert, C. A., 1990, The NO_3 radical decomposition and NO_3 scavenging in the troposphere, *J. Geophys. Res.* **95**, 13963–13969.

Flocke, F., Volz-Thomas, A., and Kley, D., 1988, Kopplung eines Chemilumineszenzdetektors mit einem Gaschromatographen zur selektiven Messung oxidierter Stickstoffverbindungen in der Atmosphäre, Berichte der KFA Jülich, Jül-2217.

Flocke, F., Volz-Thomas, A., and Kley, D., 1991, Measurement of alkyl nitrates in rural and polluted air masses, *Atmos. Environ.* **25**, 1951–1960.

Geiß, H., 1992, in preparation.

Hanson, P. J. and Lindberg, S. E., 1991, Dry deposition of reactive nitrogen compounds: a review of leaf, canopy and non-foliar measurements, *Atmos. Environ.* **25**, 1615–1634.

Heikes, B. G. and Thomson, A. M., 1983, Effects of heterogeneous processes on NO_3, HONO and HNO_3 chemistry in the troposphere, *J. Geophys. Res.* **88**, 10883–10895.

Herrmann, H., Exner, M., and Zellner, R., 1992, Laser-based studies of reactions of the nitrate radical in aqueous solution, subm. to *Ber. Bunsenges. Phys. Chem.*

Hjorth, J., Lohse, C., Nielsen, C. J., Skov, H., and Restelli, G., 1990, Products and mechanisms of the gas-phase reactions between NO_3 and a series of alkenes, *J. Phys. Chem.* **94**, 7494–7500.

Isidorov, V. A., Zenkevich, I. G., and Ioffe, B. V., 1985, Volatile organic compounds in the atmosphere of forests, *Atmos. Environ.* **19**, 1–8.

Jonston, H. S., Cantrell, C. A., and Calvert, J. G., 1986, Unimolecular decomposition of NO_3 to form NO and O_2 and review of N_2O_5/NO_3 kinetics, *J. Geophys. Res.* **91**, 1159–5172.

Kirchner, W., Welter, F., Bongartz, A., Kames, J., Schweighofer, S., and Schurath, U., 1990, Trace gas exchange kinetics at the air/water surface, *J. Atmos. Chem.* **10**, 427–449.

Klemp, D., 1992, (unpublished results).

Lamb, B., Guenther, A., Gay, D., and Westberg, H., 1987, A national inventory of biogenic hydrocarbons emissions, *Atmos. Environ.* **21**, 1695–1705.

Mellouki, A., LeBras, G., and Poulet, G., 1988, Kinetics of the reactions of NO_3 with OH and HO_2, *J. Phys. Chem.* **92**, 2229–2234.

Madronich, S., and Calvert, J. G., 1990, Permutation reaction of organic peroxy radicals in the troposphere, *J. Geophys. Res.* **95**, 5697–5715.

Mihelcic, D., Müsgen, P., and Ehhalt, D. H., 1985, An improved method of measuring tropospheric NO_2 and RO_2 by matrix isolation and electron spin resonance, *J. Atmos. Chem.* **3**, 341–361.

Mihelcic, D., Volz-Thomas, A., Pätz, H. W., Kley, D., and Mihelcic, M., 1990, Numerical analysis of ESR spectra from atmospheric samples, *J. Atmos. Chem.* **11**, 271–297.

Mozurkewich, M. and Calvert, J. G., 1988, Reaction probability of N_2O_5 on aqueous aerosols, *J. Geophys. Res.* **93**, 15889–15896.

Morris, E. D. Jr. and Niki, H., 1974, Reaction of the nitrate radical with acetaldehyde and propylene, *J. Phys. Chem.* **78**, 1337–1338.

Neta, P. and Huie, R. E., 1986, Rate constant for reactions of NO_3 radicals in aqueous solutions, *J. Phys. Chem.* **90**, 4644–4648.

Noxon, J. F., Norton, R. B., and Henderson, W. R., 1978, Observation of atmospheric NO_3, *Geophys. Res. Lett.* **5**, 675–678.

Noxon, J. F., Norton, R. B., and Marovich, E., 1980, NO_3 in the troposphere, *Geophys. Res. Lett.* **7**, 125–128.

Noxon, J. F., 1983, NO_3 and NO_2 in the mid-Pacific troposphere, *J. Geophys. Res.* **88**, 11017–11021.

Parrish, D. D., Williams, E. J., Fahey, D. W., Liu, S. C., and Fehsenfeld, F. C., 1987, Simultaneous field measurements of biogenic emissions of nitric oxide and nitrous oxide, *J. Geophys. Res.* **92**, 2165–2171.

Platt, U., Perner, D., Winer, A. M., Harris, G. W., and Pitts, J. N. Jr., 1980, Detection of NO_3 in polluted atmosphere by differential optical absorption, *Geophys. Res. Lett.* **7**, 89–92.

Platt, U., Perner, D., Schröder, J., Kessler, C., and Toenissen, A., 1981, The diurnal variation of NO_3, *J. Geophys. Res.* **86**, 11965–11970.

Platt, U., Winer, A. M., Biermann, H. W., Atkinson, R., and Pitts, J. N. Jr., 1984, Measurement of nitrate radical concentration in continental air, *Environ. Sci. Technol.* **18**, 365–369.

Platt, U., Rateike, M., Junkermann, W., Rudolph, J., and Ehhalt, D. H., 1988, New tropospheric OH measurements, *J. Geophys. Res.* **93**, 5159–5166.

Platt, U., LeBrass, G., Poulet, G., Burrows, J. P., and Moortgat, G. K., 1990, Peroxy radicals from night-time reactions of NO_3 with organics compounds, *Nature* **348**, 147–149.

Roberts, J. M., Hahn, C. J., Fehsenfeld, F. C., Warnock, J. M., Albritton, D. L., and Sievers, R. E., 1985, Monoterpene hydrocarbons in the night-time troposphere, *Environ. Sci. Technol.* **19**, 364–369.

Rudolph, J., Johnen, F. J., Khedim, A., and Pilwat, G., 1990, The use of automated 'on line' gaschromatography for the monitoring of organic trace gases in the atmosphere at low levels, *Int. J. Environ. Anal. Chem.* **38**, 143–155.

Russell, A. G., McRae, G. J., and Cass, G. R., 1985, The dynamics of nitric acid production and the fate of nitrogen oxides, *Atmos. Environ.* **19**, 893–903.

Russell, A. G., Cass, G. R., and Seinfeld, J. H., 1986, On some aspects of night-time atmospheric chemistry, *Environ. Sci. Technol.* **20**, 1167–1172.

Slemr, F., and Seiler, W., 1984, Field measurements of NO and NO_2 emissions from fertilized and unfertilized soils, *J. Atmos. Chem.* **2**, 1–24.

Sverdrup, G. M., Spicer, C. W., and Ward, G., 1987, Investigation of gas phase reaction of dinitrogen pentoxide with water vapor, *Int. J. Chem. Kin.* **19**, 191–205.

Thomas, K., 1992, PhD Thesis, Univ. Wuppertal.

Thomas, K., Kley, D., Mihelcic, D., and Volz-Thomas, A., 1989, Mass accommodation coefficient for NO_3 radicals on Water: Implication for atmospheric oxidation processes, International Conference on the generation of oxidants on regional and global scales, Norwich, 3–7 July 1989.

Volz, A., Geiß, H., McKeen, St., and Kley, D., 1989, Correlation of ozone and solar radiation at Montsouris and Hohenpeißenberg: Indications for photochemical influence, in R. D. Bojkov and P. Fabian (eds.), Ozone in the atmosphere, *Proc. Quadrennial Ozone Symposium 1988*, Deepak Publishing, Hampton, pp. 447–450.

Volz-Thomas, A., Kley, D., Pätz, H. W., Pilwat, G., Mihelcic, D., Flocke, F., and Smit, H. G. J., 1990, Local and regional ozone production: Chemistry and Transport: A contribution to the EUROTRAC subproject TOR, EUROTRAC Annual Report 1989, Part 9, pp. 57–62. International Scientific Secretariat Fraunhofer Institute IFU Garmisch-Partenkirchen.

Volz-Thomas, A., Smit, H. G. J., Kley, D., Aschmutat, U., Buers, H. J., Flocke, F., Garthe, H. J., Geiß, H., Gilge, S., Heil, T., Houben, N., Klemp, D., Loup, H., Mihelcic, D., Müsgen, P., Pätz, H. W., Pilwat, G., Sträter, W., and Su, Y., 1991, Local and regional ozone production: Chemistry and Transport: A contribution to the EUROTRAC subproject TOR, EUROTRAC Annual Report 1990, Part 9, pp. 83–94. International Scientific Secretariat Fraunhofer Institute IFU Garmisch-Partenkirchen.

Williams, E. J., Parrish, D. D., Buhr, M. P., Fehsenfeld, F. C., and Fall, R., 1988, Measurements of soil NO_x emissions in central Pennsylvania, *J. Geophys. Res.* **93**, 9539–9546.

Williams, E. J., Parrish, D. D., and Fehsenfeld, F. C., 1987, Determination of nitrogen oxide emissions from soils: results from a grassland site in Colorado, United States, *J. Geophys. Res.* **92**, 2173–2179.

Yokouchi, Y., Okaniwa, M., Ambe, A., and Fuwa, K., 1983, Seasonal variation of monoterpenes in the atmosphere of a pine forest, *Atmos. Environ.* **17**, 743–750.